Growth temperature dependence of transport properties of InAs epilayers grown on GaP

Victor Souw[a)]
Department of Physics, Purdue University, West Lafayette, Indiana 47907

V. Gopal
School of Materials Engineering, Purdue University, West Lafayette, Indiana 47907

E.-H. Chen
Department of Electrical Engineering, Yale University, New Haven, Connecticut 06520

E. P. Kvam and M. McElfresh[b)]
School of Materials Engineering, Purdue University, West Lafayette, Indiana 47907

J. M. Woodall
Department of Electrical Engineering, Yale University, New Haven, Connecticut 06520

(Received 21 December 1999; accepted for publication 23 June 2000)

Undoped InAs was grown by molecular-beam epitaxy directly on GaP at a set of different substrate temperatures. Transport properties were characterized by means of Hall-effect and resistivity measurements at temperatures between 3 and 300 K. It was observed that samples grown at higher temperatures had lower carrier concentrations, consistent with a decrease of ionized defects. In addition, samples grown at higher temperatures also had higher mobility, consistent with a smaller number of scattering centers. Samples grown at higher temperatures also showed much higher sensitivity of the mobility to the measurement temperature, suggesting a drop in neutral scattering defects. Transmission electron microscopy showed that the samples grown at higher temperatures had a significantly different dislocation microstructure. The observed dislocation microstructure is consistent with the mechanisms proposed for the influence of growth temperature on the variation of carrier concentration and mobility. © *2000 American Institute of Physics.* [S0003-6951(00)01234-1]

InAs is a narrow-gap material with the second-highest intrinsic electron mobility among the binary III–V compound semiconductors. This makes it an attractive candidate for high-speed devices and infrared optoelectronic devices. The high electron mobility also enhances the relative magnetoresistance, which makes it attractive as a magnetic-field sensing device.[1] However, the epitaxial growth of InAs necessitates the use of lattice-mismatched substrates since robust, semi-insulating InAs substrates are not available. Traditionally, InAs has been grown on GaAs substrates with a lattice mismatch of ~7%. In the present study, InAs was grown on the wide-band-gap semiconductor GaP. Although GaP has a larger lattice mismatch to InAs (~11%), it is nearly lattice matched with Si. Optimizing the growth of InAs on GaP holds the potential of integrating InAs devices with the dominant Si-based technology via GaP buffer layers. This is also a model system for fundamental studies of large-mismatch epitaxial growth, but may be important in new dielectric layer systems.

The large lattice mismatch between InAs and GaP leads to the generation of a high density of threading dislocations in the InAs layer, which can adversely affect device performance. Hence, it is useful to study carrier transport in highly dislocated InAs. We have previously described a multilayer analysis of carrier transport in InAs to account for the nonuniform threading dislocation microstructure.[2] In this letter, we focus on the influence of growth temperature on the transport properties and microstructure of InAs/GaP.

Crystal growth was performed by molecular-beam epitaxy using a Varian Gen-II system, the details of which have been reported elsewhere.[3] Each of the samples used in this study consists of an undoped 1 μm InAs layer capped by an undoped 10 nm layer of $Al_{0.2}In_{0.8}As$ in order to prevent carrier accumulation at the InAs-free surface.[2,3] The samples differed only in their growth temperature (T_g): 350, 400, and 480 °C. Hall-effect and resistivity measurements were performed in a Quantum Design PPMS system using the van der Pauw technique. Measurements were performed over the temperature range from 3 to 300 K at a magnetic field of 0.5 T, where the measured Hall voltage is linear with the magnetic field. A constant current of 25 μA was used to ensure a low electric field. Microstructural characterization was performed using a JEOL 2000 FX transmission electron microscope (TEM).

Figure 1 shows the apparent sheet carrier density (N_s) as a function of measurement temperature for the three samples. (The apparent sheet carrier concentration is defined as $N_s = IH/eV_H$. In a nonuniform sample, such as highly mismatched InAs/GaP, this apparent concentration is a weighted average of the carrier concentration and the mobility, leading to a nontrivial interpretation of the temperature dependence. For details, see Ref. 2.) A significant decrease in N_s is ob-

a)Electronic mail: vks@physics.purdue.edu
b)Also at Department of Physics, Purdue University, W. Lafayette, IN 47907.

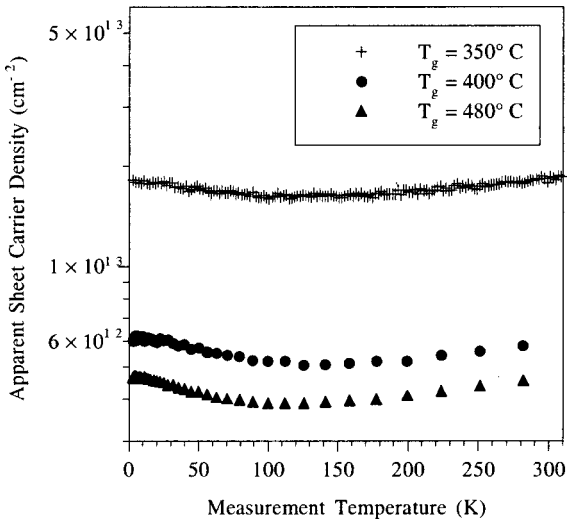

FIG. 1. Apparent sheet carrier density vs measurement temperature for samples grown at different T_g.

served at higher growth temperatures (T_g). The decrease of N_s with increased T_g suggests a decrease in the density of ionized (i.e., electrically active) defects (N_i).

Figure 2 shows the variation of apparent mobility (μ) with temperature. Three features can be seen: (1) The mobility increases with higher T_g. (2) The temperature dependence of mobility is stronger at higher T_g. (3) The maximum of the mobility shifts to lower temperatures at higher T_g.

At low measurement temperatures, the increase in μ with increasing measurement temperature suggests the predominant influence of ionized impurity/defect scattering:[4]

$$\mu_{\text{imp}} \propto \frac{T^{3/2}}{N_i}, \tag{1}$$

where N_i is the concentration of ionized defects.[4] On the other hand, above ~125 K the decrease of μ with increasing measurement temperature suggests the predominant influence of phonon (lattice) scattering:[5]

$$\mu_{\text{pho}} \propto T^{-3/2}. \tag{2}$$

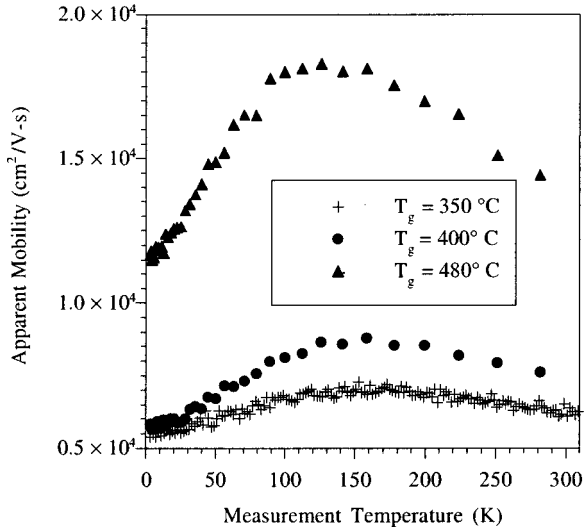

FIG. 2. Apparent electron mobility vs measurement temperature for samples grown at different T_g.

An additional, temperature-independent scattering mechanism can account for the observation that μ depends more weakly than $T^{\pm 3/2}$ on the measurement temperature at the upper and lower limits. It can also account for the observation that the dependence of μ on the measurement temperature varies for samples grown at different T_g.[2] These three scattering mechanisms combine according to

$$\mu_{\text{tot}}^{-1} = \mu_{\text{imp}}^{-1} + \mu_{\text{pho}}^{-1} + \mu_{\text{t.i.}}^{-1}. \tag{3}$$

Within this framework, the increase in mobility with T_g suggests the decrease of both ionized defect scattering and temperature-independent scattering at higher T_g. A decrease in ionized defect density would also be consistent with the decrease of carrier concentration observed in Fig. 1. In addition, the observation that μ depends more strongly on the measurement temperature at higher T_g also suggests that temperature-independent scattering decreases in samples grown at higher T_g. Finally, the shift of the mobility peak to lower temperatures at higher T_g is also consistent with a reduction of ionized defects at higher T_g. If the ionized defect density decreases at higher T_g, while the amount of phonon scattering does not, the peak or crossover point between these two competing mechanisms would shift to lower temperatures as T_g is increased.

The influence of T_g on the carrier concentration and mobility can, therefore, be qualitatively explained by a reduction of ionized defects and temperature-independent scattering in samples grown at higher T_g. It was previously suggested that temperature-independent scattering could arise from surface roughness, dislocation strain fields, and neutral defects.[2] Atomic-force microscope measurements show that the root-mean-squared roughness of the free surface is 0.9, 0.9, and 2.1 nm for the three samples grown at T_g=350, 400, and 480 °C, respectively. The samples with the smallest amount of temperature-independent scattering actually has the roughest free surface, making it unlikely that surface roughness contributes significantly to carrier scattering.

On the other hand, scattering due to dislocation strain fields would drop at higher T_g, since a small drop in the threading dislocation density is observed in TEM images. TEM images also provide evidence for other significant microstructural differences between the samples grown at different T_g. Figure 3(a) is a plan-view TEM micrograph of the InAs layer near the upper surface of the 350 °C grown sample and Fig. 3(b) that of the 480 °C grown sample. In Fig. 3(a) the standard threading dislocation contrast is seen with a density of $\sim 10^{10}\,\text{cm}^{-2}$. However, in Fig. 3(b) an additional feature is visible. The dislocation segments along the [110] direction are 90° misfit dislocations, and are confined to the $Al_{0.2}In_{0.8}As/InAs$ mismatched interface (the misfit dislocations running along $[1\bar{1}0]$ are invisible due to the particular diffraction condition).

The presence of these misfit segments indicates increased dislocation motion at higher T_g, through both glide and climb. Dislocation motion (especially climb) invariably changes the point defect concentration. The climb process activation also signifies the activation of point defect diffusion processes. A decrease in the point defect concentration,

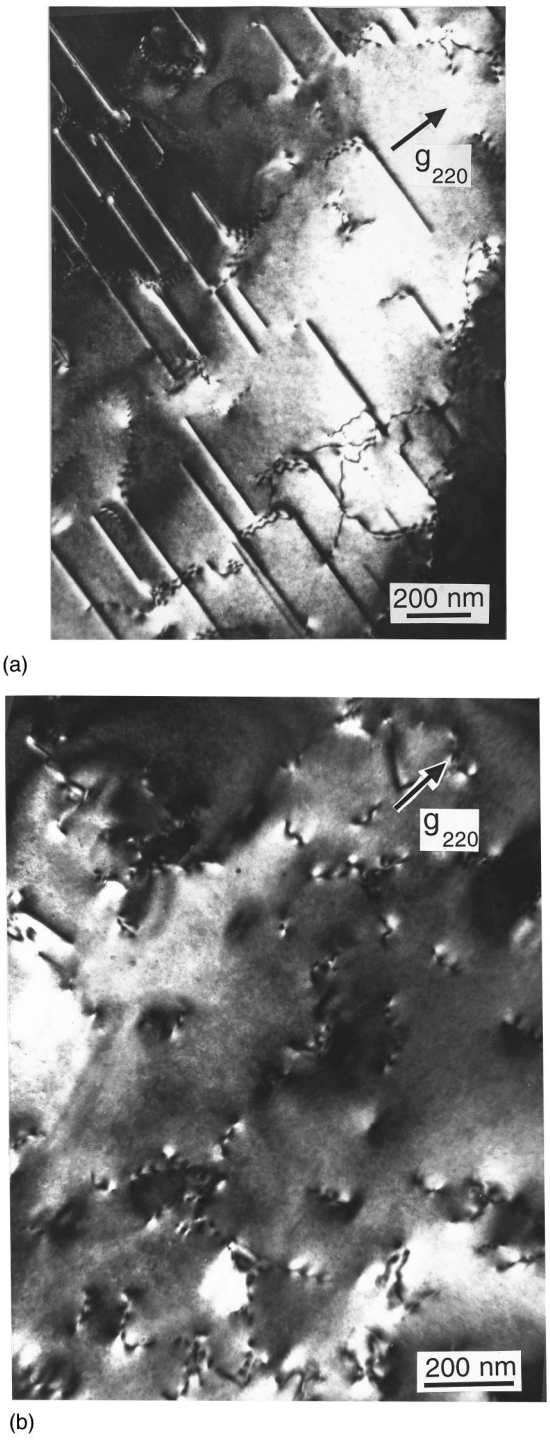

FIG. 3. Plan-view TEM micrographs of 10 nm $Al_{0.2}In_{0.8}As$/1 μm InAs/GaP heterolayers grown at (a) 350 °C and (b) 480 °C.

in turn, may be responsible for the increased mobility and its stronger dependence on measurement temperature.

The decrease of carrier concentration with increased growth temperature was previously observed by Baliga and Ghandhi in metalorganic chemical-vapor-deposition-grown InAs/GaAs.[6] They suggested that the decrease in carrier concentration resulted ultimately from the T_g dependence of the surface mobility of atoms arriving from the gas phase. The higher surface mobility led to a higher probability of point defect annihilation and, hence, to a lower concentration of point defects and carriers. However, since the melting temperature of InAs is 942 °C ($T_m = 1215$ K), growth temperatures ranging from 350 °C (623 K) to 480 °C (753 K) are sufficiently high ($T_g \geqslant 1/2T_m$) for significant bulk diffusion variations to occur as well. Hence, changes of point defect density with growth temperature could be more complicated than that suggested by Baliga and Ghandhi.[6] Specifically, processes such as pipe diffusion along threading dislocation cores are likely to become more significant at higher temperatures in this range.

Although very little is known about native defects in InAs, various possible sources have been suggested. Reinecke calculated that cation vacancies (V_{In}) contribute a midgap state and that vacancy pairs ($V_{In}-V_{As}$) result in a degenerate energy level above the conduction-band edge.[7] Positron lifetime spectroscopy also indicated the presence of neutral divacancy-type defects in InAs.[8] The occurrence of neutral antisite pairs ($In_{As}-As_{In}$) has also been postulated.[9] The equilibrium concentration of these types of point defects are a sensitive function of the growth mode and temperature. In addition, point defect densities at or near dislocations could be preferentially reduced at higher T_g. The misfit dislocations at the $Al_{0.2}In_{0.8}As$/InAs interface Fig. 3(b) suggest that significant pipe diffusion of point defects occurs at higher growth temperatures.

In conclusion, the influence of growth temperature on the transport properties and microstructure of InAs epilayers grown on GaP was investigated. The principal effects of higher growth temperatures were a reduction of the carrier density and an increase in the magnitude and measurement temperature dependence of the mobility. These effects are consistent with a reduction of charged and neutral defect densities. Such a reduction in defect densities could result from the dislocation motion and structure observed in TEM images, and also from bulk and short-circuit diffusion.

This work was partially supported by the National Science Foundation through Grant No. 9400415-DMR.

[1] J. Heremans, D. L. Partin, D. T. Morelli, B. K. Fuller, and C. M. Thrush, Appl. Phys. Lett. **57**, 291 (1990).
[2] V. Gopal, V. K. Souw, E.-H. Chen, E. P. Kvam, M. W. McElfresh, and J. M. Woodall, J. Appl. Phys. **87**, 1350 (2000).
[3] V. Gopal, E.-H. Chen, E. P. Kvam, and J. M. Woodall, J. Vac. Sci. Technol. B **17**, 1767 (1999).
[4] J. M. Ziman, *Electrons and Phonons* (Oxford University Press, London, U.K., 1962), pp. 428–438.
[5] H. Brooks, *Advances in Electronics and Electron Physics* (Academic, New York 1955), Vol. 7, p. 85.
[6] B. J. Baliga and S. K. Ghandhi, J. Electrochem. Soc. **121**, 1646 (1974).
[7] T. L. Reinecke, Physica B & C **117&118**, 194 (1983).
[8] J. Mahony and P. Mascher, Phys. Rev. B **55**, 9637 (1997).
[9] J. A. Van Vechten, J. Electrochem. Soc. **122**, 423 (1975).